

Interplay Between Wind and Rain Observed in Hurricane Floyd

In situ observations over the ocean are extremely sparse during a hurricane and conventional satellite data only provide cloud imagery at the top of the storm. Hurricanes are devastating when they are accompanied by strong winds and heavy rain. Two new satellite missions, QuikSCAT and the Tropical Rain Measuring Mission (TRMM), provide the opportunity to observe both wind and rain in hurricanes prior to landfall. The coincident measurements of surface wind and rain reveal the interplay between the dynamics and the hydrologic balances of the storms. When applied to Hurricane Floyd, the high spatial resolution of ocean surface winds measured by QuikSCAT improves computation of the moisture transport, the vertical profiles of moisture sink and diabatic heating, and the difference between evaporation and rain-rate at the surface.

The results were validated by the observations of surface rain and rain profiles by the TRMM. The close relationship between the dynamic and hydrologic parameters is visible in Figure 1 as Hurricane Floyd approaches the Bahamas on September 13, 1999. Surface winds feed moisture into the hurricane. The moisture turns into rain, releases latent heat, and fuels the storm. After the image in Figure 1 was taken, Hurricane Floyd turned north. Its strength and proximity to the Atlantic coast caused the largest evacuation of citizens in U.S. history. Landfall of Hurricane Floyd on September 16 resulted in severe flooding and devastation in the Carolinas.

A scatterometer sends microwave pulses to the Earth's surface and measures the backscatter power from the surface roughness. Over the ocean, the backscatter is largely due to small (centimeter) waves on the surface, which are believed to be in equilibrium with the local wind stress. The backscatter power depends not only on the magnitude of the wind stress, but also on the wind direction relative to the direction of the radar beam. The ability to measure wind speed and direction under both clear and cloudy conditions is what makes the scatterometer unique.

QuikSCAT was launched by NASA in June 1999 with a radar scatterometer, SeaWinds, on board [Gul et al., 1998]. SeaWinds provides a continuous 1800-km swath, thus providing over 92% coverage of the global ocean daily. The standard wind products have a 25-km resolution, but the data used in this study are

produced to have a space resolution of 12.5 km. This is significant improvement over previous scatterometers in monitoring hurricanes. The NASA Scatterometer (NSCAT), which failed in 1997, had a wide nadir-gap between two 600-km swaths, one on each side of the spacecraft, and a spatial resolution of 25 km; the data gap may prevent full coverage of a hurricane (e.g., Liu et al., 1997). The scatterometers of European Remote Sensing (ERS) satellites, which have been operating since 1992, have only a single 479-km swath and a spatial resolution of 50 km. ERS scatterometers cover only 10% of the global ocean daily and may miss large portions of hurricanes.

TRMM is joint mission of NASA and the National Space Development Agency (NASDA) of Japan. It was launched in November 1997, with a microwave imager and a precipitation radar onboard [Kummerow et al., 1998]. The microwave imager measures radiance from 10.7 GHz to 85 GHz, from which a

suite of parameters can be derived, including the surface rainfall over oceans. The spatial resolution varies with frequency, starting at 45 km at 10 GHz to 5 km at 85 GHz. The precipitation radar sends radar pulses and measures the backscatter from the atmosphere, giving TRMM the unique ability to measure the three-dimensional rainfall distribution over both land and ocean. The horizontal resolution is 4.3 km. The low-inclination orbit of TRMM is designed to give an optimal sampling rate for monitoring rainfall.

Wind, the dynamic parameter, and rain, the hydrologic parameter, are related by the principle of water and mass conservation. The influence of the ocean surface winds is not confined to the surface, but instead is felt throughout the atmospheric column. The vertical velocity in pressure coordinate at a certain level is the integral of the wind divergence at that level and all the levels below; it governs the vertical component of moisture transport. The difference between condensation and evaporation per unit mass of air at each level, called apparent moisture sink (Q) by Yanai et al. [1973], is a function of the moisture transport at that level. In convective areas, the vertical transport is particularly important, and the accuracy of surface winds

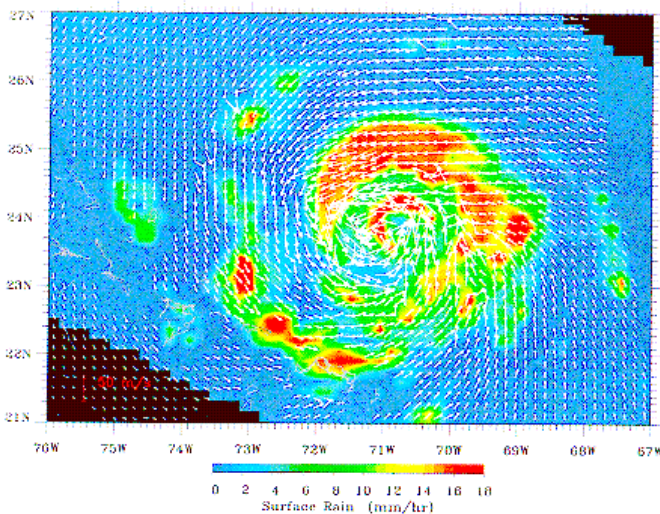


Fig. 1. Hurricane Floyd is revealed by wind vectors (white arrows) from SeaWinds and surface precipitation (color image) from the microwave imager on September 13, 1999, along the ground-tracks of QuikSCAT and TRMM, which are approximately 78 minutes apart.

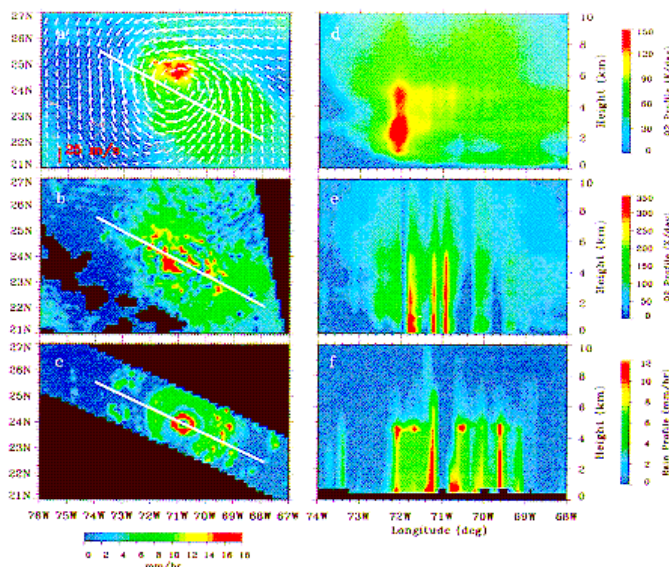


Fig. 2. Hurricane Floyd, a) as revealed by EDAS data interpolated to 10:48 UT, with white arrows representing winds at 1000 mb and the color image representing the computed air-sea fresh water flux; b) as fresh water flux computed by replacing the surface wind divergence of EDAS data with SeaWinds data that are measured at 10:48 UT; c) as surface rainfall estimated through a combination of the microwave imager and precipitation radar data at 9:30 UT. Vertical profiles of heating and rain rates along white lines in panel a), b), and c) are shown in panels d), e), and f) respectively.

affects the hydrologic balance at all levels. The profile of Q is usually expressed as the profile of diabatic heating rate per unit mass of air; $H = LQ/c$, where c is the isobaric specific heat and L is the latent heat of vaporization. The vertical integration of Q gives the air-sea fresh water flux (F), which is the difference between evaporation (E) and rain rate (R) at the surface [e.g., Bryan and Oort, 1984].

The traditional computation of H profiles and F uses wind and humidity profiles from rawinsonde. Over the ocean, rawinsonde data are sparse, and products from operational numerical weather prediction (NWP) models are used. Provided that the variation of E is small compared with R , the horizontal pattern of F and vertical pattern of H should be comparable to the surface rain pattern and vertical rain profiles measured by TRMM. By adding a wind field from the scatterometer on ERS-1, Hsu et al. [1997] improved the computation of F using the three-dimensional NWP data of the European Center of Medium Range Weather Forecast (ECMWF), in a convective region in the western tropical Pacific.

SeaWinds provides far superior coverage and resolution in describing the surface wind divergence in a hurricane than the ERS-1 scatterometer. The global ECMWF data used by Hsu et al. [1997] have 2.5° latitude by 2.5° longitude

(roughly 250 km) spatial resolution and are obviously inadequate to resolve small marine convective systems. Figure 2a shows that even with the high resolution of regional mesoscale NWP products, NWP data cannot produce realistic rain patterns for Hurricane Floyd. As demonstrated by the microwave imager data in Figure 1, Floyd has double rain bands, but the rain bands are absent in the NWP data. The NWP data are produced operationally by the Eta Data Assimilation System (EDAS) of the National Center of Environmental Prediction (NCEP). They have 40-km horizontal resolution and cover the whole U.S. mainland and the surrounding oceans.

By simply replacing the wind divergence of the EDAS data between 1000 mb and 975 mb with the divergence of scatterometer winds in the computation of F , the pattern of F shown in Figure 2b, becomes much more realistic with the appearance of more than one rain band as observed by both the microwave imager (Figure 1) and the precipitation radar (Figure 2c). Because Hurricane Floyd moves, EDAS data were linearly interpolated to the time of QuikSCAT overpass at 10:48 UT, with the spatial coordinate moving with the eye of the hurricane. At 10:48 UT, the eye of the hurricane is at 71.1° W and 23.8° N, according to the minimum value of backscatter measured by

SeaWinds. The location is consistent with the best-track analysis reported by the National Hurricane Center (NHC).

Figure 2c shows that precipitation radar, with a swath width of 220 km, has less coverage than the microwave imager swath, which is 760 km. Although there are differences between surface rain observed by the microwave imager and precipitation radar in intensity and distribution, the double circular rain bands are obvious in both. The TRMM overpass is at 9:30 a.m., earlier than SeaWinds, and the eye of Floyd is located slightly to the east. The precipitation radar provides the instant rain rate integrated over a certain atmospheric layer; vertical distribution of this rain rate should be in qualitative agreement with Q or H .

The vertical sections also show that EDAS data alone obviously do not resolve the eye nor the rain bands of the hurricane (Figure 2d). With SeaWinds data, two sharp walls of precipitation define the eye of the hurricane at 71.1° (Figure 2e). The outer rain bands passing 70.1° and 71.7° are clearly visible. The addition of scatterometer winds also increases the heating rate aloft. Precipitation radar data (Figure 2f) show the eye of Floyd at 70.9° , slightly to the east of EDAS data; the walls of the two circular rain bands are also clearly visible. Precipitation radar shows a sharp cut-off of precipitation at 5 km (Figure 2f), which may represent the freezing level. Although most of the rain is confined to below 5 km in Figure 2e, the cut off is not as dramatic.

Although the standard data products produced by the QuikSCAT Project meet the accuracy specifications in general, the accuracy under the strong wind and high rainfall conditions of a hurricane is uncertain because there are insufficient measurements for validation. Using the rain flags provided with the standard data products to discard data would eliminate most of the data in the hurricane. A semi-empirical correction algorithm that depends on wind speed and rain rate was developed using collocated backscatter measurements by SeaWinds and rain measurements by the Special Sensor Microwave Imager for seven Atlantic hurricanes in 1999. This correction is applied to produce the data set used in this study. The scatterometer wind speeds in Floyd (Figure 1) reach above 60 m/s and are comparable to a maximum value of 69.4 m/s reported by NHC. Directional errors that may be caused by rain contamination, however, still exist; these are easily identifiable in Figure 1. There are also continuous efforts in validation and algorithm improvement for TRMM.

This study shows that surface wind divergence strongly influences the hydrologic and energy balances of hurricanes. Four-dimensional assimilation of QuikSCAT and TRMM data into hurricane models in the near future will improve our understanding of this relationship and how to predict a hurricane's path. Katsaros et al. [2000, personal communication] demonstrated early detection of hurricanes by identifying rotation of surface winds

using SeaWinds, before they could be recognized in cloud motions observed from conventional satellites.

Synergistic applications of QuikSCAT and TRMM will contribute to our understanding of marine weather systems. Evolving marine weather systems can be monitored through the Seaflux Web site (<http://airsca-www.jpl.nasa.gov/seaflux>), which displays and provides access to near-real time and uniformly gridded QuikSCAT winds every 12 hours. Seaflux also includes TRMM rainfall in near-real time for selected storms.

Authors

W. Timothy Liu, Hua Hu, and Simon Yueh
Jet Propulsion Laboratory 300-323, California
Institute of Technology, Pasadena, Calif., USA

Acknowledgment

This study was performed at the Jet Propulsion Laboratory, California Institute of Technology, under contract with NASA. It was supported jointly by NASA's QuikSCAT and TRMM projects. Wenqing Tang, Carol Hsu, and Anindita Datta assisted Timothy Liu in the hurricane analysis. Whyang Tsai and Bryan Stiles worked with Simon Yueh in improving the wind-retrieval algorithm. The authors are grateful for their contributions through various stages of this study.

References

Bryan, E., and A. Cort, Seasonal variation of the global water balance based on aerological data, *J. Geophys. Res.*, **89**, 11,717–11,730, 1984.

Graf, J., C. Sasaki, C. Winn, W.T. Liu, W. Tsai, M. Freilich, and D. Long, NASA scatterometer experiment, *Acta Astronautica*, **23**, 397–407, 1993.

Hsu, C. S., W.T. Liu, and M. G. Wartels, Impact of scatterometer winds on hydrologic and convective heating through surface divergence, *Mon. Wea. Rev.*, **125**, 1556–1576, 1997.

Kummerow, C., W. Barnes, T. Kozu, J. Shiue, and J. Simpson, The Tropical Rainfall Measuring Mission (TRMM) sensor package, *J. Atmos. Oceanic Tech.*, **15**, 309–317, 1998.

Liu, W. T., W. Tang, and R. S. Dunbar, Scatterometer observes extratropical transition of Pacific typhoons, *Eos, Trans. AGU*, **78**, 237, 240, 1997.

Yanai, M., S. Esbensen, and J. H. Chu, Determination of bulk properties of tropical cloud clusters and large-scale heat and moisture budgets, *J. Atmos. Sci.*, **30**, 614–627, 1973.